Wiring of bilirubin oxidases with redox polymers on gas diffusion electrodes for increased stability of self-powered biofuel cells-based glucose sensing

Jana M Becker, Anna Lielpetere, Julian Szczesny, Sabrina Bichon, Sébastien Gounel, Nicolas Mano, Wolfgang Schuhmann

Bioelectrochemistry 149 (2023) 108314

Contents lists available at ScienceDirect

Bioelectrochemistry

journal homepage: www.journals.elsevier.com/bioelectrochemistry

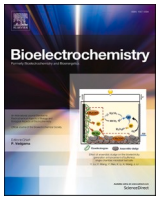

Wiring of bilirubin oxidases with redox polymers on gas diffusion electrodes for increased stability of self-powered biofuel cells-based glucose sensing

Jana M. Becker [a], Anna Lielpetere [a], Julian Szczesny [a], Sabrina Bichon [b], Sébastien Gounel [b], Nicolas Mano [b], Wolfgang Schuhmann [a,*]

[a] Analytical Chemistry – Center for Electrochemical Sciences (CES), Faculty of Chemistry and Biochemistry, Ruhr-University Bochum, Universitätsstraße 150, D-44780 Bochum, Germany

[b] Centre de Recherche Paul Pascal, CNRS UMR 5031, University of Bordeaux, Avenue Albert Schweitzer, 33600 Pessac, France

ARTICLE INFO

Keywords:
Bilirubin oxidase
Glucose sensor
Gas diffusion electrode
Oxygen reduction
Redox polymer

ABSTRACT

A new redox polymer/bilirubin oxidase (BOD)-based gas diffusion electrode was designed to be implemented as the non-current and non-stability limiting biocathode in a glucose/O_2 biofuel cell that acts as a self-powered glucose biosensor. For the proof-of-concept, a bioanode comprising the Os-complex modified redox polymer P(VI-*co*-AA)-[Os(bpy)$_2$Cl]Cl and FAD-dependent glucose dehydrogenase to oxidize the analyte was used. In order to develop an optimal O_2-reducing biocathode for the biofuel cell *Mv*-BOD as well as *Bp*-BOD and *Mo*-BOD have been tested in gas diffusion electrodes in direct electron transfer as well as in mediated electron transfer immobilized in the Os-complex modified redox polymer P(VI-*co*-AA)-[Os(diCl-bpy)$_2$]Cl$_2$. The resulting biofuel cell exhibits a glucose-dependent current and power output in the concentration region between 1 and 10 mM. To create a more realistic test environment, the performance and long-term stability of the biofuel cell-based self-powered glucose biosensor has been investigated in a flow-through cell design.

1. Introduction

Glucose has a critical role as the main energy source for living organisms. Metabolic disorders, like diabetes, in which the glucose level in the body is disturbed, have vast impacts on the quality of life for the people affected [1].

Wearable devices that offer continuous control of blood glucose levels demand the integration of an energy source, not only for the detection of glucose but also for signal transmission to a read-out or smart device [2]. However, the use of batteries to provide the necessary energy can act as a bottleneck in the miniaturization of such devices. Hence, self-powered systems are an attractive approach for miniaturized sensors for continuous glucose quantification. A self-powered glucose biosensor based on a biofuel cell (BFC) comprising an anode based on a flavin adenine dinucleotide (FAD) tethered to pyrrolo quinoline quinone (PQQ) reconstituted with the apo-enzyme of glucose oxidase for glucose oxidation and a cathode modified with cytochrome *c*/cytochrome oxidase for O_2 reduction was first reported in 2001 [3]. Immobilization and electrical connection of glucose converting enzymes in BFC-based glucose sensors has been common practice since it has first been shown by the research group of A. Heller [4,5].

However, the reductive counter reaction to the glucose oxidation plays an equally important role in the development of self-powered, long-term stable glucose sensors. The oxygen reduction reaction (ORR) is a straightforward choice since the substrate (O_2) is readily available in ambient conditions. A device with an anode based on glucose oxidase wired and immobilized in an Os-complex modified redox polymer for glucose oxidation and a Pt/C modified cathode for O_2 reduction has first been reported by Feldman et al. [6].

An alternative to noble metal-based catalysts for oxygen reduction are biocatalysts such as multi-copper oxidases which exhibit large turnover rates for the reduction of molecular oxygen into water. Such biocatalysts for the ORR like bilirubin oxidase (BOD) can be wired either in direct electron transfer (DET) or mediated electron transfer (MET). In DET systems, the biocatalyst communicates directly with the electrode material *via* electron tunnelling. One major limitation of DET systems is the fact that only a monolayer of enzymes with the correct anisotropic orientation towards the electrode can be efficiently wired directly to the

* Corresponding author.
E-mail address: wolfgang.schuhmann@rub.de (W. Schuhmann).

https://doi.org/10.1016/j.bioelechem.2022.108314
Received 23 August 2022; Received in revised form 15 October 2022; Accepted 21 October 2022
Available online 27 October 2022

electrode since the electron transfer rate decreases exponentially with an increased distance for electron tunnelling [7]. In MET, a redox mediator that acts as an electron shuttle between the enzyme and the electrode material is used and allows for electrical wiring of more than a monolayer of enzymes irrespective of their orientation [8].

Various approaches have been reported on how to improve enzyme orientation and enzyme loading of BOD in DET by increasing the electroactive surface area of the electrode and improving the interaction between electrode material and redox protein [8]. Examples are the use of carbon nanostructures like pristine or chemically modified single-walled [9] and multi-walled [10] carbon nanotubes, graphene [11], carbon nanoparticles like Vulcan [12] and Ketjen Black [13] or gold nanostructures like Au nanoparticles [14] or self-assembled monolayers [15].

The electron transfer and catalyst loading limitations arising in DET can be circumvented by wiring the biocatalyst in MET. Various redox mediators, e.g. 2,2′-azinobis(3-ethylbenzothioazolin-6-sulfonate) (ABTS), promazine, hydroquinone syringaldazine and ferrocyanide have been reported to electrically wire multi-copper oxidases to glassy carbon electrodes [16]. In 1998, Leech et al. were the first to report the use of an Os-complex as a redox mediator for O_2 reduction to water catalysed by multi-copper oxidases [17]. Os-complexes are particularly versatile redox mediators as their potential can be adjusted to be close to that of the biocatalyst by exchanging the ligands around the Os-centre [18,19]. The use of a redox polymer in which the redox mediator is covalently attached to a polymer backbone does not only provide mediator species for efficient electron transfer but can also act as an immobilization matrix for the enzyme [5,20].

Even when large quantities of the biocatalyst were electrically wired and immobilized, currents are typically still limited by slow diffusion of the gaseous substrate O_2. Hence, making the cathodic reaction non-current limiting is of particular importance because the current output of the fuel cell should be directly correlated to the glucose concentration of the sample to allow for quantification of the analyte. Therefore, low current densities at the cathode limit the miniaturization of a self-powered glucose biosensor since a large surface area cathode for O_2 reduction would be necessary.

While methods of forced convection like rotating disk electrodes are unpractical for application in a device, an elegant way to increase current densities limited by the diffusion of gaseous substrates without need for additional energy is the use of gas diffusion electrodes (GDEs). In a GDE, a three-phase boundary is established at the interface between liquid electrolyte, solid electrode/catalyst material and gaseous substrate. The quick dissolution of the gas into a thin layer of electrolyte formed around the catalyst material due to the large concentration gradient between gaseous and aqueous phase and shortened diffusion pathways leads to an increased local O_2 flux at the catalyst site and hence, higher catalytic currents [21,22]. Due to these advantages, GDEs have been well established in the development of fuel cells and electrolysers since their implementation in 1932 [21] and have gained increasing interest in the field of bioelectrocatalysis as well [22].

Here, we present a comparison between three different kinds of bilirubin oxidases embedded in a redox polymer on gas diffusion electrodes as high-current density biocathodes for O_2 reduction for application in a biofuel cell assembly with a flavin adenine dinucleotide dependent glucose dehydrogenase (FAD-GDH)/Os-complex modified redox polymer-based bioanode in a long-term stable glucose/O_2 biofuel cell that acts as a self-powered glucose sensor.

2. Methods

2.1. Chemicals

All chemicals were purchased from Sigma-Aldrich, Merck, Acros Organics, abcr, Alfa Aesar, J.T. Baker, Fisher Chemicals or VWR and were of reagent or higher grade.

2.2. Enzymes

FAD-GDH was prepared as described in reference [23] and stored at −30 °C. Bilirubin oxidase from *Myrothecium verrucaria* (*Mv*-BOD) was purchased from Sigma Aldrich and stored at −20 °C. BOD from *Bacillus pumilus* (*Bp*-BOD) and from *Magnaporthe oryzae* (*Mo*-BOD) were isolated, produced, purified as previously reported [24,25] and stored at −80 °C before use.

2.3. Electrochemical measurements

All electrochemical measurements were performed using a Gamry Reference 1000 potentiostat at room temperature. When half-cell experiments in a 3-electrode setup were performed, a Ag/AgCl/3 M KCl reference electrode (RE) was used, and a Pt-wire acted as counter electrode (CE). Characterization of the biocathode was performed in a gas diffusion cell as described in reference [26]. While Ar was bubbled into the phosphate buffer electrolyte (0.1 M, pH 7.3), either the gaseous substrate (O_2) or an inert gas (Ar) were provided to the back of the gas diffusion electrode. For measurements in the flow-through cell, the cell was assembled as shown in Fig. 5 and S1. A gold wire was attached to the carbon cloth bioelectrodes for electrical connection. The electrolyte flow rate was adjusted to 5 μL s^{-1}.

2.4. Synthesis of (redox) polymers

For the synthesis of poly(vinylimidazole-*co*-acrylamide)-[Os(dichlorobipyridine)$_2$Cl]Cl (P(VI-*co*-AA)-[Os(diCl-bpy)$_2$]Cl$_2$), 15 mL of ethylene glycol were deaerated in a Schlenk flask. 163.7 mg Os(4,4′-dichloro-2,2′-bipyridine)$_2$-dichloride (Os(II)(diCl-bpy)$_2$Cl$_2$, synthesized according to [27]) and poly(vinylimidazole-*co*-acrylamide (105 mg, synthesized according to [28]) were added. To dissolve the polymer backbone, the solution was heated to 60 °C for 25 min. For the reaction, the solution was heated to 180 °C for 2 h in an argon atmosphere. After 2 h the solution was cooled down to room temperature and Et_2O/acetone (240 mL/60 mL) was added. The clear supernatant was decanted off and the precipitate was dissolved in MeOH (1. 15 mL, 2. 20 mL) and precipitated again by adding Et_2O (400 mL each time). The procedure was repeated 2 times until the supernatant was colorless. Finally, the dark red product was dried in an oven (75 °C) overnight, yielding 139.3 mg (51.8 wt%). The resulting solid was dissolved in H_2O and filtered, leading to an aqueous solution with a polymer concentration of 15.8 mg mL^{-1}.

Poly(1-vinylimidazole-co-acryl hydrazide)-[Os(2,2′bipyridine)$_2$Cl]Cl (P(VI-*co*-AA)-[Os(bpy)$_2$Cl]Cl) was synthesized according to a previously published procedure [29]. Poly(styrene sulfonate-*co*-glycidyl methacrylate-*co*-butylacrylate) (P(SS-GMA-BA)) was synthesized in a free radical polymerisation according to the procedure from [30].

2.5. Biocathode preparation

Before modification, the carbon cloth ($d = 2$ cm) was first rinsed with ethanol and subsequently with H_2O. After drying shortly, the electrode was modified. Modification with enzyme for direct electron transfer was carried out by drop-casting 20 μL of an enzyme solution (10 mg mL^{-1}) directly onto the carbon cloth and drying overnight at 4 °C. For experiments employing the redox polymer P(VI-*co*-AA)-[Os(diCl-bpy)$_2$]Cl$_2$ to wire the enzyme to the electrode surface, first an underlying polymer layer was deposited to exclude any possibility of a directly wired enzyme. For this, 17 μL P(VI-*co*-AA)-[Os(diCl-bpy)$_2$]Cl$_2$ (15.8 mg mL^{-1}) were drop-casted onto the electrode surface. The active layer, composed of 17 μL P(VI-*co*-AA)-[Os(diCl-bpy)$_2$]Cl$_2$ (15.8 mg mL^{-1}) and 20 μL BOD (10 mg mL^{-1}), was immobilized on top of the dried underlying redox polymer layer. After each deposition step, the electrodes were left to dry overnight at 4 °C. The carbon cloth electrodes were only partially modified, covering an area of 0.2 cm^2 ($d = 5$ mm) both in DET and MET.

2.6. Bioanode preparation

The carbon cloth was rinsed with ethanol and subsequently with water. After drying shortly at ambient conditions, an aqueous solution of P(VI-*co*-AA)-[Os(bpy)$_2$Cl]Cl (11 μL, 12.3 mg mL^{-1}) was drop-casted onto the macroporous side of the carbon cloth (d = 2 cm), modifying an area of ca. 0.2 cm^2 (d = 5 mm). The electrode was left to dry overnight in the fridge (4 °C). The active layer was prepared by mixing of 11 μL of P(VI-*co*-AA)-[Os(bpy)$_2$Cl]Cl solution (12.3 mg mL^{-1}), 6.8 μL FAD-GDH solution (15 mg mL^{-1}) and 1.7 μL poly(ethylene glycol) diglycidyl ether (PEGDGE, 1:40 dilution with H_2O) and subsequent drop-casting on top of the dried adhesion layer. After drying overnight at 4 °C, the capping layer was added by drop-casting a mixture of 17 μL P(SS-GMA-BA) solution (60 mg mL^{-1}) and 1.7 μL of 2,2′-(ethylenedioxy)diethylamine (EDEA) on top of the already deposited layers and the electrode was dried overnight at 4 °C again.

3. Results and discussion

At the biocathode of the proposed self-powered biofuel cell-based glucose sensor, a carbon cloth gas diffusion layer was used as the electrode material to overcome diffusional limitation of the gaseous substrate O_2. Oxygen-reducing bilirubin oxidase was immobilized inside the Os-complex modified redox polymer P(VI-*co*-AA)-[Os(diCl-bpy)$_2$]Cl$_2$ (E = 0.57 V vs SHE) that has previously been proven to efficiently wire BOD to electrode surfaces [19,24], allowing for increased catalyst loading and improved electron transfer and therefore, larger catalytic currents compared to the enzyme wired in DET. Furthermore, its high redox potential allows maximizing of the open circuit voltage (OCV), when implemented as cathode in a BFC. FAD-GDH was employed as catalyst at the bioanode for glucose oxidation to glucono-δ-lactone due to its good stability and high substrate selectivity [31]. The enzyme was embedded into the Os-complex modified redox polymer P(VI-*co*-AA)-[Os(bpy)$_2$Cl]Cl exhibiting a midpoint potential of 0.43 V vs SHE. Since the FAD-GDH, similarly to glucose oxidase, has a deeply buried cofactor, DET is not feasible [32]. The used Os-complex is known to wire glucose converting enzymes for electrochemical applications [33]. The used polymer backbone contains a hydrazide crosslinking group to allow for more stable polymer films. To further improve film stability on the electrode surface, an additional redox silent capping layer, consisting of P(SS-GMA-BA) was added on top of the substrate-converting layer. The epoxy group of the redox silent polymer can also react with the hydrazide group of the redox polymer providing a covalent attachment between the layers (Fig. 1).

3.1. Biocathode

For the development of a long-term stable glucose-sensing biofuel cell, a non-current-limiting biocathode with good stability is crucial. Since the electrochemical response is linked to the catalytic performance of the enzyme, different bilirubin oxidases were compared in MET as well as in DET to obtain an electrode with optimal current output and long-term stability. The three bilirubin oxidases were the commercially available high redox potential yeast *Mv*-BOD (670 mV vs SHE [8]), as well as the thermostable low redox potential bacterial *Bp*-BOD (630 mV vs SHE [24]) and the high redox potential yeast *Mo*-BOD (690 mV vs SHE [34]). Voltammetric experiments under non-turnover (Fig. 2A) and turnover conditions electrodes (Fig. 2B) modified with *Mv*-BOD (Fig. 2, black lines) and *Bp*-BOD (Fig. 2, red lines) in DET showed poor average catalytic current responses of 23 ± 6 μA (n = 3) and 5 ± 1 μA (n = 3). Surprisingly, the capacitive current is higher for both yeast BODs compared to the bacterial one, which may be due to glycosylation. In long-term amperometric experiments under turnover conditions, electrodes modified with *Mv*-BOD and *Bp*-BOD both reached 50 % of their initial current value after an approximate average of 8 ± 1 h (n = 3) (Fig. S2 A & B). On the other hand, electrodes modified with *Mo*-BOD in DET (Fig. 2, green lines) exhibited a significantly higher current response with an average of 350 ± 70 μA (n = 3) for the ORR and half of the initial catalytic current was reached only after an average of 20 ± 6 h (n = 3) (Fig. S3) indicating superior catalytic performance and long-term stability of the *Mo*-BOD when wired in DET regime on the used electrode material when no additional surface modification is performed.

The catalytic current response could be significantly enhanced for all three enzymes by immobilization in the redox polymer P(VI-*co*-AA)-[Os(diCl-bpy)$_2$]Cl$_2$. This effect can be attributed to a more efficient electron transfer enabled by the mediator species attached to the redox polymer and the three-dimensional wiring of a higher number of enzyme molecules. While cyclic voltammetry (CV) under non-turnover conditions shows similar redox signals from the redox polymer regardless of the employed enzyme with the exception of a lower capacitive current for *Mo*-BOD (Fig. 3 A), a significant difference was observed for the catalytic current responses when O_2 was offered to the backside of the GDE.

In MET, the *Bp*-BOD exhibited an average catalytic current response of 175 ± 66 μA (n = 3) (Fig. 3 B, red line), while the *Mv*-BOD reached an average of 430 ± 125 μA (n = 3) (Fig. 3 B, black line), and *Mo*-BOD an even higher average current of 580 ± 100 μA (n = 3) (Fig. 3 B, green line). It has to be pointed out that the enzyme activity as determined for a dissolved enzyme is not necessarily the same as for the enzyme embedded within the redox polymer. The turnover rate is governed by a complex interplay of local substrate availability, the intrinsic properties

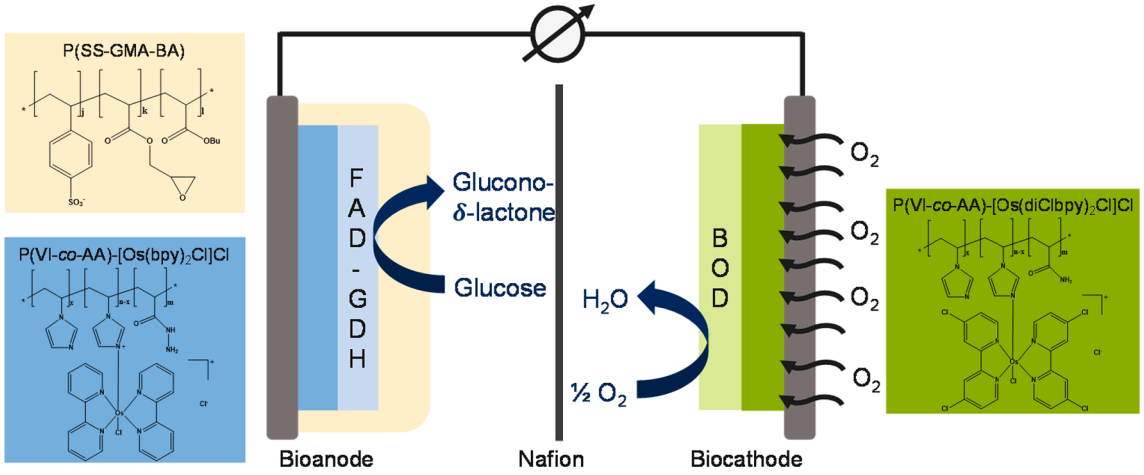

Fig. 1. Schematic representation of the self-powered glucose/O_2 biofuel cell-based glucose sensor.

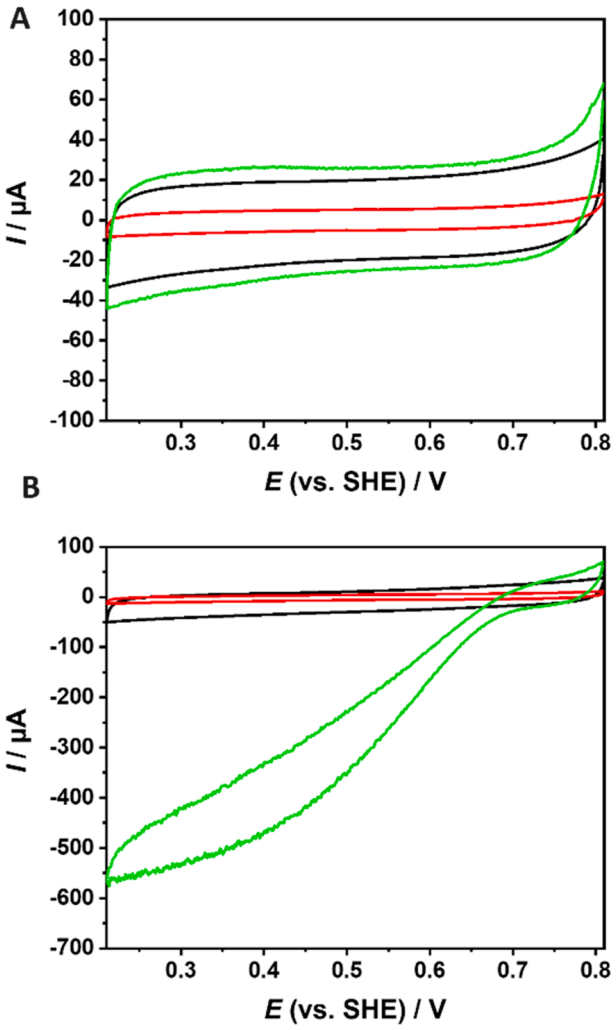

Fig. 2. Voltammetric characterization of electrodes modified with *Mv*-BOD (black lines), *Bp*-BOD (red lines) and *Mo*-BOD (green lines) in direct electron transfer regime under Ar atmosphere (A) and with O_2 provided at the backside of the GDE (B). Electrolyte: 0.1 M phosphate buffer (pH 7.3), enzyme loading = 0.2 mg, $\nu = 5$ mV s^{-1}.

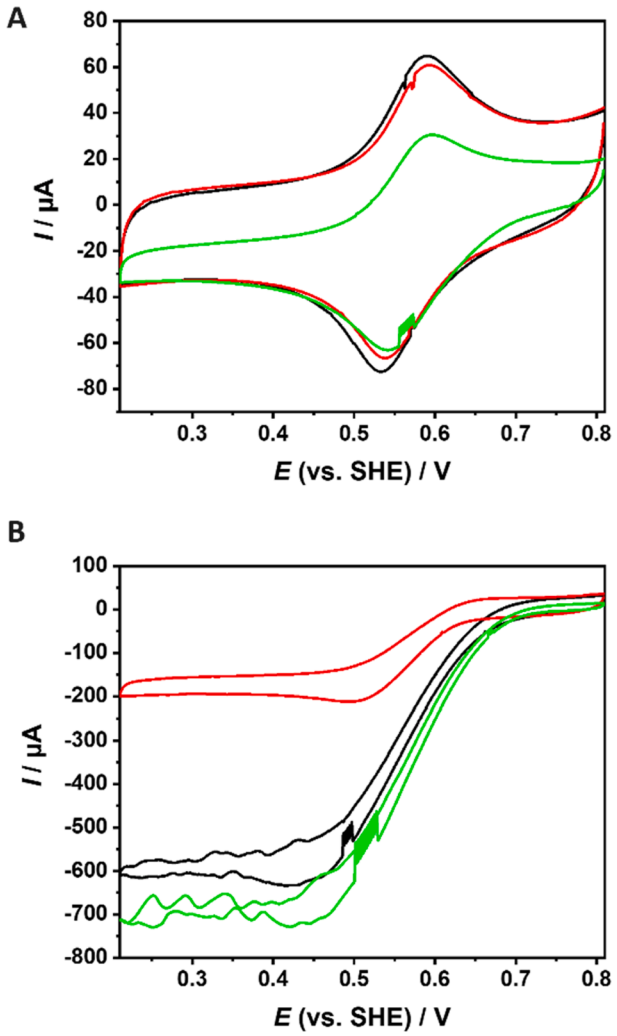

Fig. 3. Voltammetric characterization of electrodes modified with P(VI-*co*-AA)-[Os(diCl-bpy)$_2$]Cl$_2$ and *Mv*-BOD (black lines), *Bp*-BOD (red lines) and *Mo*-BOD (green lines) under Ar atmosphere (A) and with O_2 provided at the backside of the GDE (B). Electrolyte: 0.1 M phosphate buffer (pH 7.3), enzyme loading = 0.2 mg, polymer loading = 0.54 mg, $\nu = 5$ mV s^{-1}.

of the used enzyme, the electron-transfer rate between polymer-tethered Os-complex and the T1 site inside the enzyme as well as the rate of the electron hopping within the polymer. Hence, an enzyme which may exhibit a higher intrinsic activity may not show an increased current if the electron transfer rate between the T1 Cu site and the Os-complex is smaller due to a lower formal potential difference. The differences in the observed catalytic current, which is lowest for the case of Bp-BOD, can hence be attributed to the difference in driving force between the T1 Cu of the three BODs and the redox potential of the Os-complex-modified polymer. Additionally, the influence of the T1 Cu redox potential on the catalytic current response can be observed with regard to the over-potential of the catalytic current which is lowest for *Mo*-BOD, followed by *Mv*-BOD, and *Bp*-BOD.

Compared to experiments with these enzymes immobilized on a rotating disk electrode with the same Os-complex modified redox polymer, absolute catalytic ORR currents on GDEs were about 4 times larger for *Bp*-BOD [24], 40 times larger for *Mv*-BOD [19], and 6 times larger for *Mo*-BOD [19], respectively. This confirms that diffusional mass transport limitations can be largely overcome by means of a GDE. While currents for *Mv*-BOD and *Bp*-BOD increased 19- and 35-fold respectively in MET, currents for the *Mo*-BOD only increased by approximately 65 % when the enzyme was embedded in the redox polymer. Although this is still a major current increase, it indicates that *Mo*-BOD is significantly more prone to undergo efficient DET on the used electrode material when compared to the other two enzymes leaving less room for improvement regarding electron transfer rates and amount of wired biocatalyst by utilization of a redox polymer.

In long-term chronoamperometric experiments, electrodes modified with the redox polymer P(VI-*co*-AA)-[Os(diCl-bpy)$_2$]Cl$_2$ and the respective bilirubin oxidase, showed an increased stability compared to electrodes modified only by drop-casting with the enzymes in DET. Electrodes modified with *Mv*-BOD reached 50 % of their initial catalytic current value after an average of 30 ± 8 h in MET (Fig. S4A), while electrodes modified with *Bp*-BOD were stable for 60 ± 25 h (Fig. S4B). *Mo*-BOD in MET showed a similar long-term stability like *Bp*-BOD, with an average of 60 ± 5 h until 50 % of the initial catalytic current was reached (Fig. S4C). The long-term stability has been significantly improved for electrodes with the enzymes embedded within the redox polymer compared to operating the same enzyme on a non-premodified electrode in DET. Furthermore, the values are at least similar to the highest stability values found for a BOD under continuous turnover on a GDE [22,35].

Cyclic voltammograms of the modified electrodes performed under non-turnover conditions before and after long-term electrolysis indicate

that the redox polymer film remains stable on the time scale of the long-term experiments with only a minor decrease in the peak currents of the Os-complex redox wave regardless of the enzyme (Fig. S5). Thus, electrode stability must be limited either by the intrinsic stability of the respective enzyme or by enzyme leaking out of the polymer film during the experiments.

Altogether, the MET results are consistent with the intrinsic properties of the different BODs. The current of *Bp*-BOD is lower than that of *Mv*-BOD because the redox potential of the T1 is lower in *Bp*-BOD, decreasing the driving force between the T1 Cu site and the redox polymer. *Bp*-BOD is more thermostable than *Mv*-BOD, and an electrode made with *Bp*-BOD therefore exhibits improved long-term stability. The current obtained with *Mo*-BOD is higher than that of *Mv*-BOD because the enzyme is more active and twice as stable because *Mo*-BOD is more thermostable than *Mv*-BOD.

3.2. Bioanode

For the bioanode, FAD-GDH was immobilized on the electrode surface using the Os-complex modified redox polymer P(VI-*co*-AA)-[Os(bpy)$_2$Cl]Cl and an additional capping layer of P(SS-GMA-BA). The enzyme could be efficiently wired as an oxidative catalytic current can be observed in the corresponding cyclic voltammogram after adding glucose to the electrolyte (Fig. 4, red curve).

Since quantification of an analyte with an amperometric electrochemical sensor requires a linear relation between analyte concentration and current response, a chronoamperometric experiment with increasing glucose concentrations was performed to determine the linear detection range for the bioanode. The electrode was tested in glucose concentrations between 1 and 100 mM (Fig. S6A). Concentrations were increased after a steady state current was obtained for the previous glucose concentration. The resulting calibration curve (Fig. S6B) displays a linear range between 1 and 10 mM glucose. The bioanode allows for glucose quantification in human blood in which glucose concentrations are expected to be in a range of 3 to 10 mM [36].

3.3. Biofuel cell

Finally, the behavior of the complete biofuel cell-based glucose sensor was investigated in a flow-through cell design (Fig. 5) to simulate conditions closer to potential applications. The flow-through cell consists of two electrolyte compartments, separated by a Nafion membrane (Fig. 5 & S1).

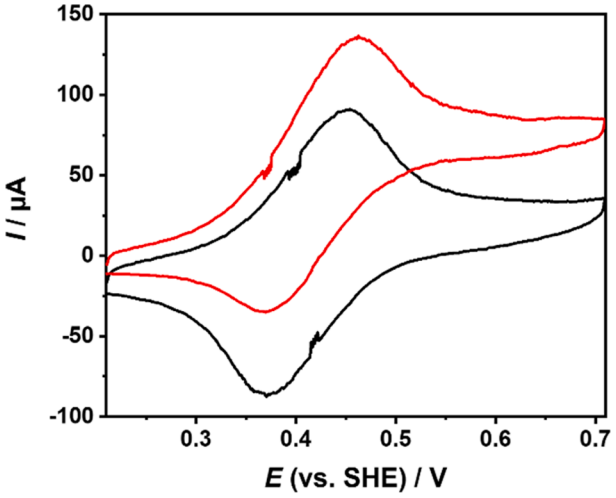

Fig. 4. Voltametric characterization of an electrode modified with the redox polymer P(VI-*co*-AA)-[Os(bpy)$_2$Cl]Cl, FAD-GDH and P(SS-GMA-BA) in 0.1 M phosphate buffer (black curve) and 0.1 M phosphate buffer containing 10 mM glucose (red curve). Enzyme loading: 0.1 mg, polymer loading: 0.28 mg P(VI-*co*-AA)-[Os(bpy)$_2$Cl]Cl and 1 mg P(SS-GMA-BA), $\nu = 5$ mV s^{-1}.

While the biocathode is operating under passive air-breathing conditions in a stationary solution, the bioanode is exposed to a continuous electrolyte flow. For independent investigation of anode and cathode in a three-electrode setup, external reference and counter electrodes can be introduced into the flow-through cell. The biofuel cell exhibited an OCV of 500 mV. Current and power curves of the BFC (Fig. 6A & B) were derived from multi-step chronoamperometric experiments of the BFC at different glucose concentrations. The biofuel cell showed an increase in current and power with increasing glucose concentration with the maximum power output at a cell voltage of 250 mV, indicating that the bioanode is indeed the current limiting electrode. Therefore, the glucose concentration in the electrolyte directly correlates with the power output of the biofuel cell.

The current response of the biofuel cell at a cell voltage of 250 mV was monitored while switching the electrolyte between phosphate buffer and phosphate buffer containing different glucose concentrations ranging from 2.5 to 15 mM (Fig. 7A). As expected, the current increases with the amount of glucose in the electrolyte and returns to the background when the glucose concentration was 0 mM, indicating that no glucose accumulates inside the polymer film of the bioanode.

From the resulting calibration curve (Fig. 7B), a linear current to glucose concentration is observed up to a concentration of 10 mM. For concentrations significantly larger than 10 mM the catalytic current saturates. These results are in line with the results obtained for the bioanode and neither the biocathode reaction nor flow-through conditions have a negative impact on the bioanode.

The long-term stability of the biofuel cell based self-powered glucose biosensor was investigated under continuous turnover conditions (250 mV cell voltage, 10 mM glucose) in the flow-through cell and the 50 % value of the initial power output was reached after approximately 24 h (Fig. 8). After stabilizing, the power output remained at the same level for another 28 h.

Investigation of the individual electrodes of the BFC by means of CV revealed that the stability of the BFC was limited by the stability of the bioanode while the current output of the cathode remained well above that of the anode (Fig. S7A & B). Linear extrapolation of the long-term stability data of the biocathode indicates that catalytic currents that would compromise the glucose quantification ability of the device are only reached after approximately 280 h. The proposed biocathode based on the redox polymer P(VI-*co*-AA)-[Os(diCl-bpy)$_2$]Cl$_2$ and *Mo*-BOD is highly suitable for application in a long-term stable self-powered glucose sensor.

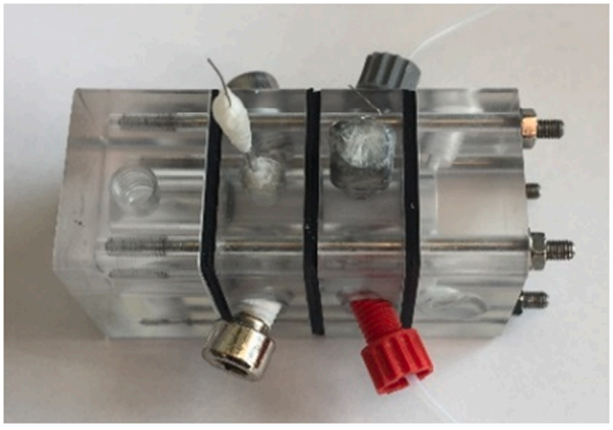

Fig. 5. Photograph of the flow-through cell. A schematic illustration can be found in the supporting information (Fig. S1).

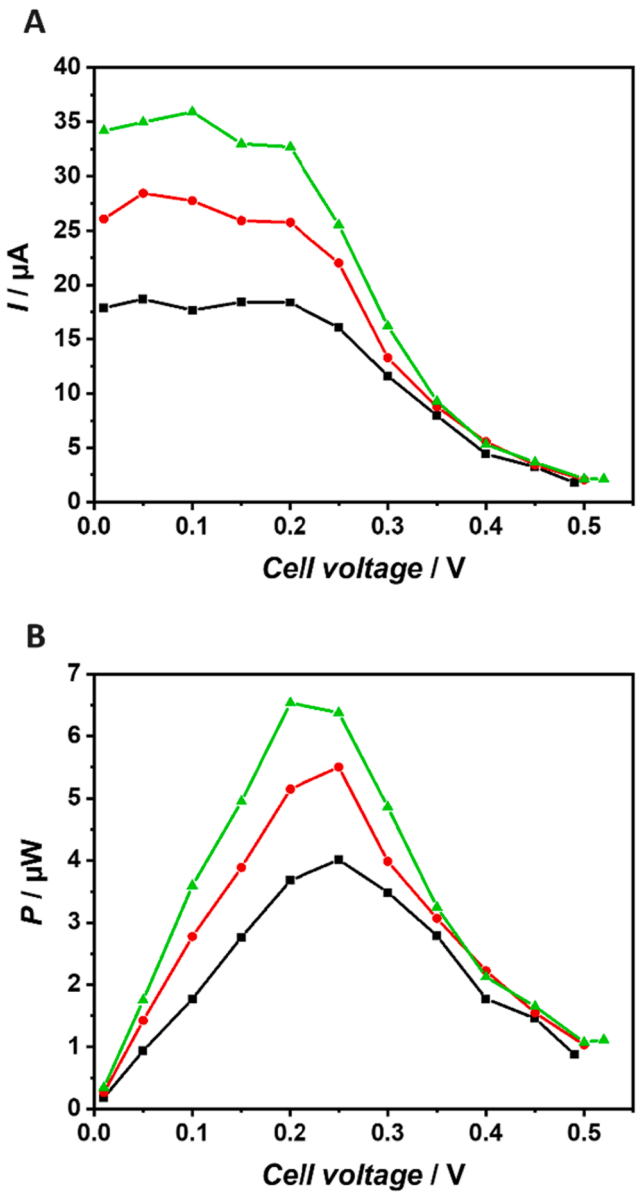

Fig. 6. Current (A) and power curves (B) of the biofuel cell with a biocathode comprising the redox polymer P(VI-*co*-AA)-[Os(diCl-bpy)$_2$]Cl$_2$ and *Mo*-BOD and a bioanode modified with the redox polymer P(VI-*co*-AA)-[Os(bpy)$_2$Cl]Cl, FAD-GDH and P(SS-GMA-BA). The curves were derived from a multi-step chronoamperometric measurement starting at the OCV of 500 mV and decreasing the cell voltage in 100 mV steps after a steady state current was reached. Electrolyte: 0.1 M phosphate buffer containing 5 mM (black), 8 mM (red) and 10 mM (green) glucose using the flow-through cell. Biocathode: Enzyme loading: 0.2 mg, polymer loading: 0.54 mg. Bioanode: Enzyme loading: 0.1 mg, polymer loading: 0.28 mg P(VI-*co*-AA)-[Os(bpy)$_2$Cl]Cl and 1 mg P(SS-GMA-BA).

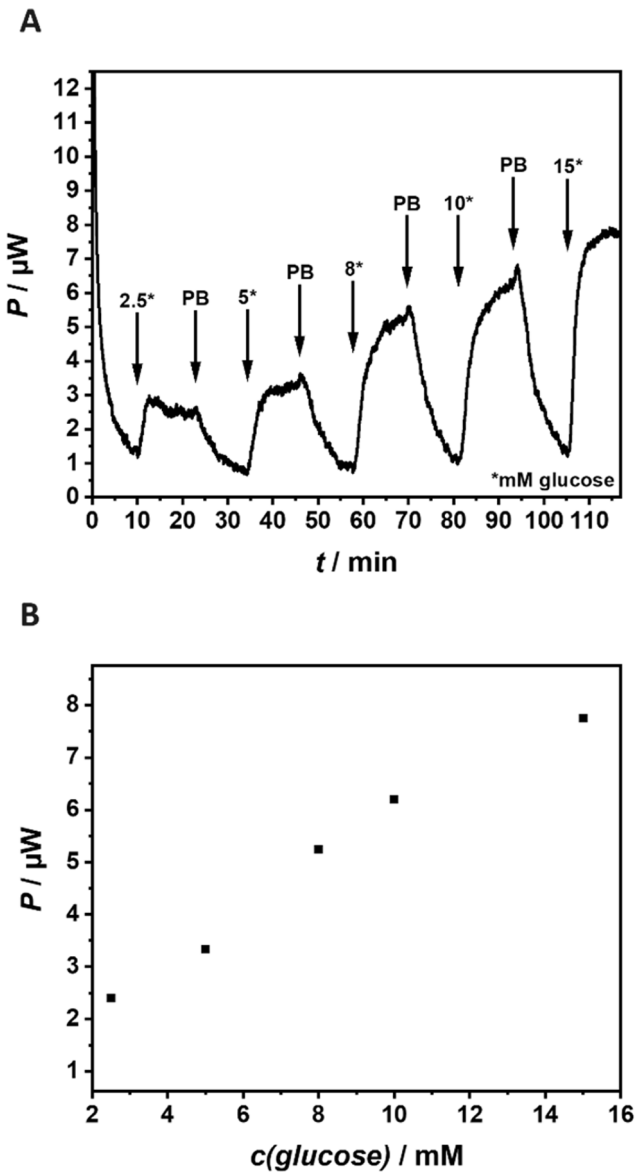

Fig. 7. (A) Power of the biofuel cell-based glucose sensor with a biocathode comprising the redox polymer P(VI-*co*-AA)-[Os(diCl-bpy)$_2$]Cl$_2$ and *Mo*-BOD and a bioanode modified with the redox polymer P(VI-*co*-AA)-[Os(bpy)$_2$Cl]Cl, FAD-GDH and P(SS-GMA-BA) at a constant cell voltage of 250 mV. The electrolyte in the flow-through cell was switched between phosphate buffer and phosphate buffer containing different glucose concentrations from 2.5 to 15 mM. Biocathode: enzyme loading: 0.2 mg, polymer loading: 0.54 mg. Bioanode: enzyme loading: 0.1 mg, polymer loading: 0.28 mg P(VI-*co*-AA)-[Os(bpy)$_2$Cl]Cl and 1 mg P(SS-GMA-BA). (B) Calibration curve of the sensor derived from power output in (A) at different glucose concentrations.

4. Conclusion

Comparison of different BODs immobilized on gas diffusion electrodes in DET as well as in MET shows superior performance of *Mo*-BOD in comparison to *Mv*-BOD and *Bp*-BOD towards the ORR and long-term stability. Current output and stability of the bioelectrodes were significantly improved by immobilization of the biocatalyst in the Os-complex modified redox polymer P(VI-*co*-AA)-[Os(diCl-bpy)$_2$]Cl$_2$. Therefore, the designed bioelectrode for the ORR comprising the redox polymer P(VI-*co*-AA)-[Os(diCl-bpy)$_2$]Cl$_2$ and *Mo*-BOD is an ideal candidate for implementation as the cathode in a self-powered biofuel cell-based glucose sensor. When combined with a glucose-converting bioanode based on FAD-GDH and the low potential Os-complex modified redox polymer P(VI-*co*-AA)-[Os(bpy)$_2$Cl]Cl quantitative glucose detection in the concentration range of 1 to 10 mM was achieved. This proof of concept could be used as the basis for a minimal invasive device for continuous glucose monitoring where the biocathode is exposed to air above the skin of a patient for the ORR while the bioanode is confined within a needle which is inserted into the patient for glucose oxidation.

Declaration of Competing Interest

The authors declare the following financial interests/personal relationships which may be considered as potential competing interests:

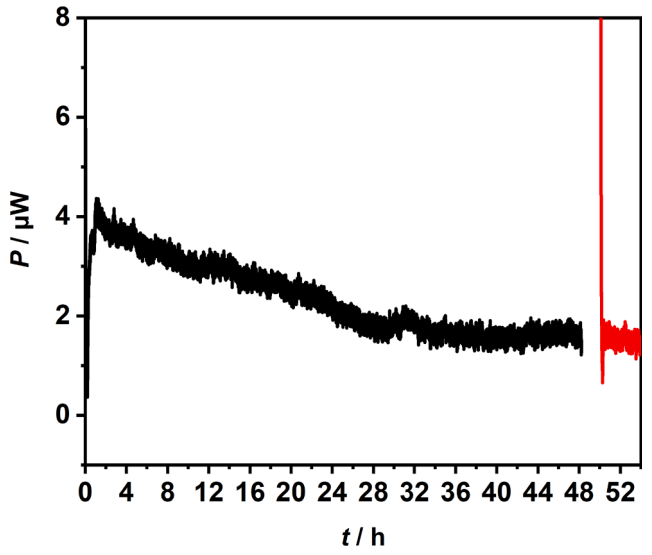

Fig. 8. Long-term experiment of the biofuel cell in the flow-through cell in 0.1 M phosphate buffer (pH 7.3) containing 10 mM glucose. Cell voltage: 250 mV. Note: The long-term measurement was interrupted to perform voltametric characterization of the electrodes after 48 h. Hence, the times of two consecutive amperometric measurements with the same electrode were added up on the x-axis. Start of the second chronoamperometry is indicated by change of color from black to red.

'Wolfgang Schuhmann reports financial support was provided by European Commission.'

Data availability

Data will be made available on request.

Acknowledgements

The authors are grateful to Prof. Dr. R. Ludwig, BOKU - University of Natural Resources and Life Sciences, Vienna; for the provision of the FAD-GDH. We acknowledge funding from the Deutsche Forschungsgemeinschaft (DFG, German Research Foundation) in the framework of the SPP2240 (e-biotech) [445820469] and the European Union's Horizon 2020 research and innovation program under the Marie Skłodowska-Curie MSCA-ITN "ImplantSens" [813006].

Appendix A. Supplementary material

Supplementary data to this article can be found online at https://doi.org/10.1016/j.bioelechem.2022.108314.

References

[1] S. Dagogo-Jack (Ed.), Springer EBook Collection Medicine, Springer, Cham, Switzerland, 2017.
[2] a) A.J. Bandodkar, J. Wang, Electroanalysis 28 (2016) 1188–1200;
b) I. Jeerapan, J.R. Sempionatto, J. Wang, Adv. Funct. Mater. 30 (2020) 1906243.
[3] E. Katz, A.F. Buckmann, I. Willner, J. Am. Chem. Soc 123 (2001) 10752–10753.
[4] a) A. Heller, Acc. Chem. Res. 23 (1990) 128–134;
b) A. Heller, Curr. Opin. Chem. Biol. 10 (2006) 664–672.
[5] A. Heller, J. Phys. Chem. 96 (1992) 3579–3587.
[6] Z. Liu, B. Cho, T. Ouyang, B. Feldman, Anal. Chem. 84 (2012) 3403–3409.
[7] a) C.C. Page, C.C. Moser, X. Chen, P.L. Dutton, Nature 402 (1999) 47–52;
b) R.A. Marcus, Angew. Chem. Int. Ed. 32 (1993) 1111–1121.
[8] N. Mano, A. de Poulpiquet, Chem. Rev. 118 (2018) 2392–2468.
[9] a) A. Ciaccafava, A. de Poulpiquet, V. Techer, M.T. Giudici-Orticoni, S. Tingry, C. Innocent, E. Lojou, Electrochem. Commun. 23 (2012) 25–28;
b) D. Ivnitski, K. Artyushkova, P. Atanassov, Bioelectrochem. 74 (2008) 101–110;
c) F. Gao, Y. Yan, L. Su, L. Wang, L. Mao, Electrochem. Commun. 9 (2007) 989–996;
d) X. Li, L. Zhang, L. Su, T. Ohsaka, L. Mao, Fuel Cells 9 (2009) 85–91;
e) A. Korani, A. Salimi, Biosens. Bioelectron. 50 (2013) 186–193.
[10] a) K. Schubert, G. Goebel, F. Lisdat, Electrochim. Acta 54 (2009) 3033–3038;
b) M. Weigel, E. Tritscher, F. Lisdat, Electrochem. Commun. 9 (2007) 689–693;
c) Y. Ogawa, K. Kato, T. Miyake, K. Nagamine, T. Ofuji, S. Yoshino, M. Nishizawa, Adv. Healthc. Mater. 4 (2014) 506–510;
d) S. Krishnan, F.A. Armstrong, Chem. Sci. 3 (2012) 1015.
[11] C. Di Bari, A. Goñi-Urtiaga, M. Pita, S. Shleev, M.D. Toscano, R. Sainz, A.L. de Lacey, Electrochim. Acta 191 (2016) 500–509.
[12] A. Habrioux, T. Napporn, K. Servat, S. Tingry, K.B. Kokoh, Electrochim. Acta 55 (2010) 7701–7705.
[13] a) C. Santoro, S. Babanova, B. Erable, A. Schuler, P. Atanassov, Bioelectrochem. 108 (2016) 1–7;
b) J. Filip, J. Tkac, J. Biotechnol. 185 (2014) S21–S22;
c) I. Shitanda, S. Kato, Y. Hoshi, M. Itagaki, S. Tsujimura, Chem. Commun. 49 (2013) 11110.
[14] a) X. Wang, M. Falk, R. Ortiz, H. Matsumura, J. Bobacka, R. Ludwig, M. Bergelin, Lo Gorton, S. Shleev, Biosens. Bioelectron. 31 (2012) 219–225;
b) D. Pankratov, R. Sundberg, D.B. Suyatin, J. Sotres, A. Barrantes, T. Ruzgas, I. Maximov, L. Montelius, S. Shleev, RSC Adv. 4 (2014) 38164–38168;
c) K. Monsalve, M. Roger, C. Gutierrez-Sanchez, M. Ilbert, S. Nitsche, D. Byrne-Kodjabachian, V. Marchi, E. Lojou, Bioelectrochem. 106 (2015) 47–55.
[15] a) T.X.H. Le, M. Bechelany, A.B. Engel, M. Cretin, S. Tingry, Electrochim. Acta 219 (2016) 121–129;
b) T. Siepenkoetter, U. Salaj-Kosla, X. Xiao, S. Belochapkine, E. Magner, Electroanalysis 28 (2016) 2415–2423.
[16] C. Fernández-Sánchez, T. Tzanov, G.M. Gübitz, A. Cavaco-Paulo, Bioelectrochem. 58 (2002) 149–156.
[17] F. Daigle, F. Trudeau, G. Robinson, M.R. Smyth, D. Leech, Biosens. Bioelectron. 13 (1998) 417–425.
[18] N. Mano, F. Mao, A. Heller, J. Electroanal. Chem. 574 (2005) 347–357.
[19] M. Cadet, X. Brilland, S. Gounel, F. Louerat, N. Mano, ChemPhysChem 14 (2013) 2097–2100.
[20] a) A. Heller, *Electrical Wiring of Redox Enzymes Photochemical Conversion and Storage of Solar Energy*, **1990**, Springer Netherlands, can be found under, doi: 10.1007/978-94-011-3396-8_5; b) Y. Degani, A. Heller, J. Amer. Chem. Soc. 111 (1989) 2357–2358; c) B.A. Gregg, A. Heller, J. Phys. Chem. 95 (1991) 5970–5975; d) A. Ruff, Curr. Opin. Electrochem. 5 (2017) 66–73; e) M. Yuan, S.D. Minteer, Curr. Opin. Electrochem. 15 (2019) 1–6.
[21] S. Park, J.-W. Lee, B.N. Popov, Int. J. Hyd. Energy 37 (2012) 5850–5865.
[22] K. So, K. Sakai, K. Kano, Curr. Opin. Electrochem. 5 (2017) 173–182.
[23] C. Sygmund, P. Staudigl, M. Klausberger, N. Pinotsis, K. Djinović-Carugo, D. Lo Gorton, R.L. Haltrich, Microb. Cell Fact. 10 (2011) 1–9.
[24] F. Durand, C.H. Kjaergaard, E. Suraniti, S. Gounel, R.G. Hadt, E.I. Solomon, N. Mano, Biosens. Bioelectron. 35 (2012) 140–146.
[25] F. Durand, S. Gounel, C.H. Kjaergaard, E.I. Solomon, N. Mano, Appl. Microbiol. Biotechnol. 96 (2012) 1489–1498.
[26] J. Szczesny, N. Marković, F. Conzuelo, S. Zacarias, I.A.C. Pereira, W. Lubitz, N. Plumeré, W. Schuhmann, A. Ruff, Nat. Commun. 9 (2018) 1–9.
[27] S. Alsaoub, F. Conzuelo, S. Gounel, N. Mano, W. Schuhmann, A. Ruff, ChemElectroChem 6 (2019) 2080–2087.
[28] T. de Lumley-Woodyear, P. Rocca, J. Lindsay, Y. Dror, A. Freeman, A. Heller, Anal. Chem. 67 (1995) 1332–1338.
[29] M. Marquitan, M.D. Mark, A. Ernst, A. Muhs, S. Herlitze, A. Ruff, W. Schuhmann, J. Mater. Chem. B 8 (2020) 3631–3639.
[30] F. Lopez, S. Ma, R. Ludwig, W. Schuhmann, A. Ruff, Electroanalysis 29 (2017) 154–161.
[31] M.N. Zafar, N. Beden, D. Leech, C. Sygmund, R. Ludwig, Lo Gorton, Anal. Bioanal. Chem. 402 (2012) 2069–2077.
[32] a) J. Wang, Electroanalysis 13 (2001) 983–988;
b) P.N. Bartlett, F.A. Al-Lolage, J. Electroanal. Chem. 819 (2018) 26–37;
c) J. Wang, Chem. Rev. 108 (2008) 814–825;
d) G. Kenausis, Q. Chen, A. Heller, Anal. Chem. 69 (1997) 1054–1060;
e) W. Schuhmann, Rev. Mol. Biotech. 82 (2002) 425–441;
f) R.A. Marcus, N. Sutin, Biochim. Biophys. Acta 811 (1985) 265–322;
g) H. Yoshida, G. Sakai, K. Mori, K. Kojima, S. Kamitori, K. Sode, Sci. Rep. (2015) 5.
[33] M. Marquitan, T. Bobrowski, A. Ernst, P. Wilde, J. Clausmeyer, A. Ruff, W. Schuhmann, J. Electrochem. Soc. 165 (2018) G3008.
[34] S. Gentil, M. Carrière, S. Cosnier, S. Gounel, N. Mano, A. Le Goff, Chem Eur. J. 24 (2018) 8404–8408.
[35] a) J. Tang, X. Yan, W. Huang, C. Engelbrekt, J.Ø. Duus, J. Ulstrup, X. Xiao, J. Zhang, Biosens. Bioelectron. 167 (2020), 112500;
b) K. Yamagiwa, Y. Ikeda, K. Yasueda, Y. Handa, N. Yabuuchi, S. Komaba, J. Electrochem. Soc. 162 (2015) F1425.
[36] G. Danaei, M.M. Finucane, Y. Lu, G.M. Singh, M.J. Cowan, C.J. Paciorek, J.K. Lin, F. Farzadfar, Y.-H. Khang, G.A. Stevens, et al., Lancet 378 (2011) 31–40.